

## Supplementary material

### Glycerol hydrogenolysis to 1,2 propanediol over novel Cu/ZrO<sub>2</sub> catalysts

Giuseppina Luciani<sup>1</sup>, Giovanna Ruoppolo<sup>2</sup>, Gianluca Landi<sup>2\*</sup>, Valentina Gargiulo<sup>2</sup>, Michela Alfè<sup>2</sup>, Almerinda Di Benedetto<sup>1</sup>

<sup>1</sup> Dipartimento di Ingegneria Chimica, dei Materiali e della Produzione Industriale, Univ. of Naples Federico II, P.le V. Tecchio 80, 80125 Naples, Italy; giuseppina.luciani@unina.it; almerinda.dibenedetto@unina.it.

<sup>2</sup> Institute of Sciences and Technologies for Sustainable Energy and Mobility-CNR, P.le V. Tecchio 80, 80125 Naples, Italy; giovanna.ruoppolo@stems.cnr.it; gianluca.landi@stems.cnr.it; valentina.gargiulo@stems.cnr.it; michela.alfe@stems.cnr.it.

\*Correspondence: gianluca.landi@stems.cnr.it; Tel.: +39-0817682235

#### **Table of contents**

Section S1: Additional characterization of catalysts precursors, as-prepared and used catalysts.

Table S1: Elemental analysis of fresh and used samples. Error is calculated with respect to the theoretical Cu content; Cu loss is calculated with respect to the actual Cu content in the corresponding fresh sample.

Figure S1: XRD analysis of MOF(HKUST-1)-Zr(C) and Cu(M)-Zr(C) samples.

Figure S2. SEM micrograph of MOF(HKUST-1)-Zr(C) (left panel) and its corresponding O, Zn, Cu combined EDS map (right panel).

Figure S3. SEM micrograph of Cu(M)-Zr(C) (left panel) and its corresponding O, Zn, Cu combined EDS map (right panel).

Figure S4: TG in air environment on MOF(HKUST-1), MOF(HKUST-1)-Zr(C) and Cu(M)-Zr(C) samples.

Section S2: Fluid dynamics and mass transfer calculations

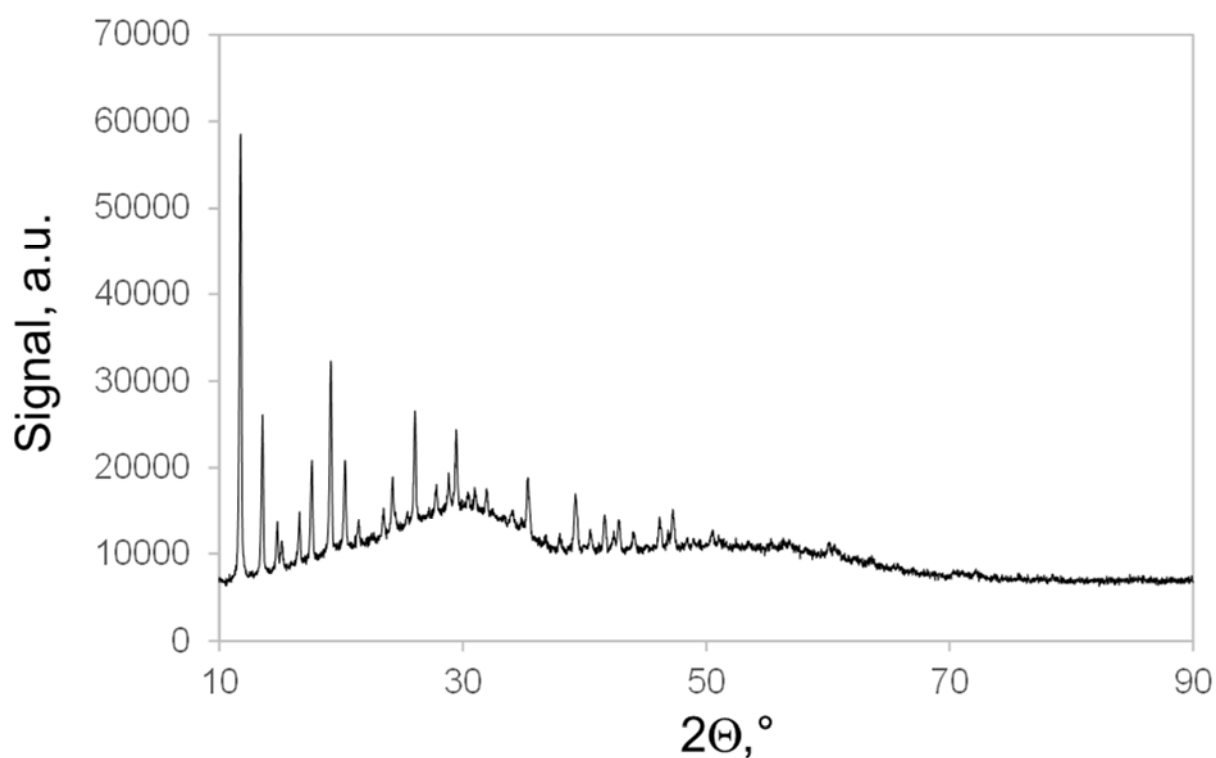
Table S2: values used for calculations.

Table S3: results of calculations.

**Section S1: Additional characterization of catalysts precursors, as-prepared and used catalysts.**

**Table S1: Elemental analysis of fresh and used samples. Error is calculated with respect to the theoretical Cu content; Cu loss is calculated with respect to the actual Cu content in the corresponding fresh sample.**

Sample	Cu content (fresh)	Error (%)	Cu content (used)	Cu loss (%)
Cu(I)-Zr(C)	11.4	-4.7	11.1	2.8
Cu(I)-Zr(S)	11.8	-1.3	11.6	1.9
Cu(M)-Zr(C)	12.2	2.0	12.3	-1.4
Cu(M)-Zr(S)	12.4	3.3	12.0	3.1



**Figure S1: XRD analysis of MOF(HKUST-1)-Zr(C).**

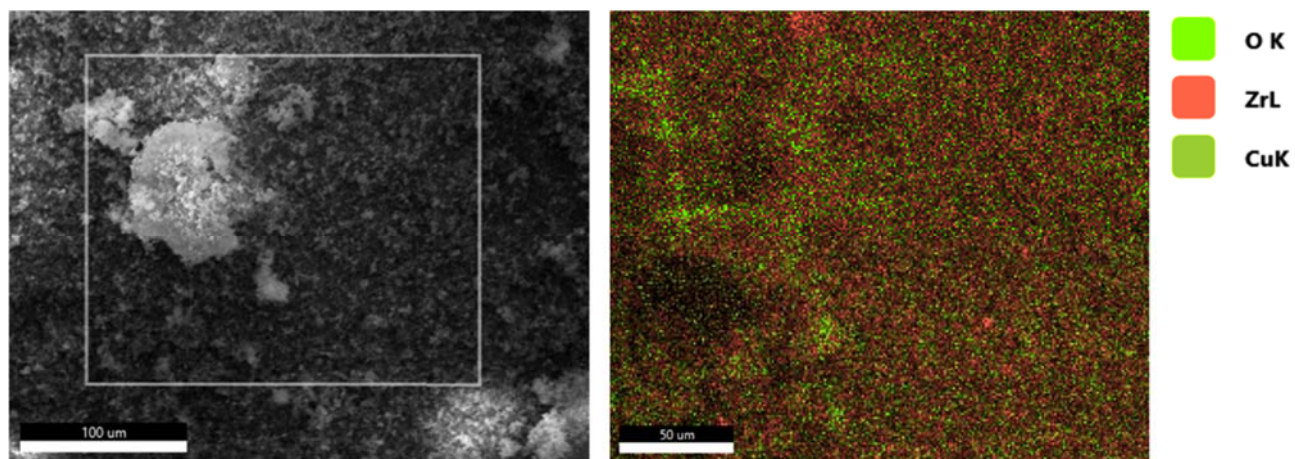


Figure S2. SEM micrograph of MOF(HKUST-1)-Zr(C) (left panel) and its corresponding O, Zn, Cu combined EDS map (right panel).

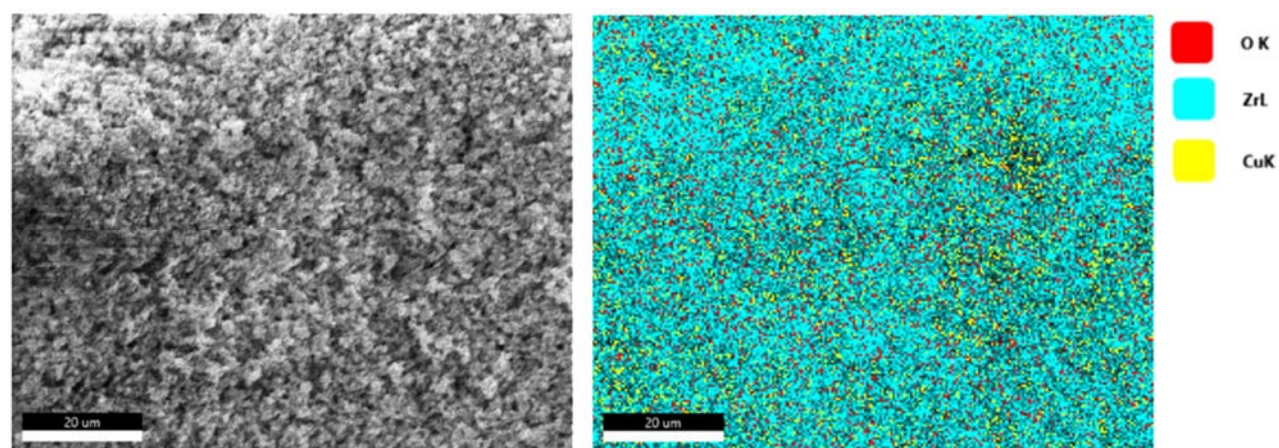


Figure S3. SEM micrograph of Cu(M)-Zr(C) (left panel) and its corresponding O, Zn, Cu combined EDS map (right panel).

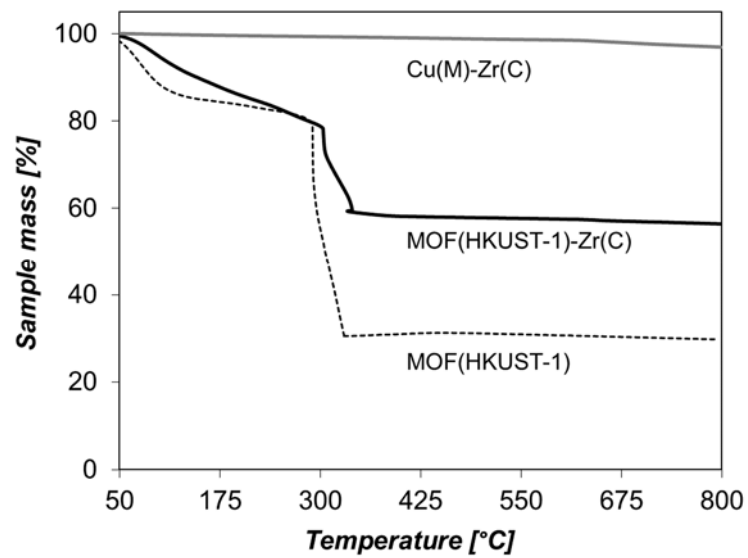


Figure S4: TG in air environment on MOF(HKUST-1), MOF(HKUST-1)-Zr(C) and Cu(M)-Zr(C) samples.

## Section S2. Fluid dynamics and mass transfer calculations

Information about fluid dynamics and mass transfer limitations in the catalytic fixed bed placed inside the PARR reactor (see Section 4.3) were derived according to the procedure reported below.

The PARR reactor is provided with a torque sensor, measuring the torque needed to keep the desired rotation speed. In particular, the instrument furnishes the required voltage fraction; at full load, the torque is equal to 1.76 Nm and the motor requires 0.125 hp (equal to 0.093 kW). By considering the typical dimension of particles ( $125 < d_p < 300 \mu\text{m}$ ) with respect to those of the channels of the flow guide, the pressure drops of the channels can be considered negligible with respect to those of the catalytic bed. Accordingly, the net motor work can be:

$$W = \Delta P \cdot F \quad (1)$$

Where  $W$  is the net motor work,  $\Delta P$  is the pressure drop and  $F$  is the flow rate through the catalytic bed. Moreover, flow rate and pressure drops are linked for a packed bed by the Ergun equation:

$$\left( \frac{\Delta P \cdot \rho}{G_0^2} \right) \cdot \frac{d_p}{L} \cdot \frac{\varepsilon^3}{1 - \varepsilon} = 150 \cdot \frac{1 - \varepsilon}{(d_p \cdot G_0 / \mu)} + 1.75 \quad (2)$$

Where  $\rho$  is the fluid density,  $G_0$  is the mass velocity (i.e. mass flow rate/cross section of the catalyst bed),  $d_p$  is the mean particle size,  $L$  is the catalyst bed length,  $\varepsilon$  is the bed void fraction,  $\mu$  is the fluid viscosity. Table S2 and S3 show the values used for calculations and the results respectively. Due to the low glycerol content, fluid properties were assumed equal to water ones.

In order to calculate the external mass transfer coefficient, the Chilton-Colburn equations were used:

$$j_D = \frac{k_c}{u} \cdot Sc^{2/3} \quad (3)$$

$$j_D = \frac{0.99}{Re^{0.41}} \quad Re > 350 \quad (4)$$

$$j_D = \frac{1.82}{Re^{0.51}} \quad Re < 350 \quad (5)$$

Where  $j_D$  is the Chilton-Colburn factor,  $k_c$  is the mass transfer coefficient,  $u$  is the fluid velocity,  $Sc$  is the Schmidt number,  $Re$  is the Reynolds number.  $Re$  and  $Sc$  number are defined:

$$Re = \frac{G_0 \cdot d_p}{\mu} \quad (6)$$

$$Sc = \frac{\mu}{\rho \cdot D_{AB}} \quad (7)$$

Where  $D_{AB}$  is the diffusivity of glycerol (or hydrogen) in water. For the glycerol diffusivity, the value reported by Rausch et al. [1] at 0.299 mol fraction and 422 K was used. By considering that diffusivity increases by decreasing the glycerol concentration and by increasing the temperature, the used value is an underestimation. About hydrogen diffusivity, the value reported in [2] was used. The highest investigated temperature was 35 °C. According to the above considerations, also this value is an underestimation. Table S2 shows the values used for calculations.

Under the hypothesis of external mass transfer limitation (i.e. fast reaction kinetics), the reaction rate is equal to external mass transfer:

$$r = k_c \cdot a_v \cdot c_R \quad (8)$$

Where  $a_v$  is the external specific surface area and  $c_R$  is the limiting reactant concentration. Accordingly, conversion ( $x$ ) is equal to

$$x = 1 - e^{-k_c \cdot a_v \cdot t} \quad (9)$$

Where  $t$  is the reaction time in a batch reactor. Table S3 shows the results of the above calculations at 500 and 1000 rpm respectively.

As reported in Table S3, external mass transfer is fast enough to guarantee complete conversion of the limiting reactant independently from the limiting species.

**Table S2: values used for calculations.**

Parameter	Definition	Value	Units
D	Diameter of the catalytic bed	2.3	cm
S	Area of the cross section of the bed	4.15	cm <sup>2</sup>
L	Length of the catalytic bed	2.9	cm
V	Volume of the catalytic bed	12	cm <sup>3</sup>
$d_p$	Mean particle size	200	μm
$a_v$	External specific surface area	30000	m <sup>-1</sup>
$\epsilon$	Bed void fraction	0.5	
$\rho$	Liquid density	1000	Kg/m <sup>3</sup>
$\mu$	Liquid viscosity	0.01	cP
$D_{AB}$	Diffusivity of glycerol in water	$4.12 \cdot 10^{-9}$	m <sup>2</sup> /s
$D_{AB}$	Diffusivity of glycerol in water	$6.31 \cdot 10^{-9}$	m <sup>2</sup> /s
$W_{max}$	Max motor power	0.125	hp

**Table S3: results of calculations.**

Parameter	Definition	Value @ 500 rpm	Value @ 1000 rpm	Units
W	Net motor power	4.66	28.9	W
$\Delta P$	Pressure drop	0.66	1.99	bar
F	Flow rate	$7.05 \cdot 10^{-5}$	$1.45 \cdot 10^{-4}$	m <sup>3</sup> /s
Re	Reynolds number	33.9	69.8	
Sc	Schmidt number	243	243	
$j_D$	Chilton-Colburn factor	0.30	0.21	
$k_c$	Mass transfer coefficient	$1.31 \cdot 10^{-3}$	$1.87 \cdot 10^{-3}$	m/s
x	Glycerol conversion under mass transfer limitations	1	1	
x	Hydrogen conversion under mass transfer limitations	1	1	

## References

1. Rausch, M. H.; Heller, A.; Fröba, A. P. Binary Diffusion Coefficients of Glycerol-Water Mixtures for Temperatures from 323 to 448 K by Dynamic Light Scattering. *J. Chem. Eng. Data* **2017**, 62, 4364–4370.
2. Engineering ToolBox Gases Solved in Water - Diffusion Coefficients  
[https://www.engineeringtoolbox.com/diffusion-coefficients-d\\_1404.html](https://www.engineeringtoolbox.com/diffusion-coefficients-d_1404.html) (accessed Dec 15, 2021).